UC Irvine
UC Irvine Previously Published Works

Title
Coordination chemistry within a protein host: regulation of the secondary coordination sphere

Permalink
https://escholarship.org/uc/item/4xd2266r

Journal
Chemical Communications, 54(35)

ISSN
1359-7345

Authors
Mann, Samuel I
Heinisch, Tillmann
Ward, Thomas R
et al.

Publication Date
2018-04-26

DOI
10.1039/c8cc01931b

Peer reviewed

eScholarship.org Powered by the California Digital Library
University of California

Author Manuscript
Author Manuscript
Author Manuscript
Author Manuscript

HHS Public Access
Author manuscript
Chem Commun (Camb). Author manuscript; available in PMC 2018 May 09.

Published in final edited form as:
Chem Commun (Camb). 2018 April 26; 54(35): 4413–4416. doi:10.1039/c8cc01931b.

Coordination chemistry within a protein host: regulation of the secondary coordination sphere[†]

Samuel I. Mann[a], **Tillmann Heinisch**[b], **Thomas R. Ward**[b], and **A. S. Borovik**[a]

[a]Department of Chemistry, 1102 Natural Science II, University of California, Irvine, CA 92697, USA [b]Department of Chemistry, University of Basel, Mattestrasse 24a, BPR 1096, CH 4002 Basel, Switzerland

Abstract

Secondary coordination spheres of metal complexes are instrumental in controlling properties that are linked to function. To study these effects in aqueous solutions artificial Cu proteins have been developed using biotin–streptavidin (Sav) technology and their binding of external azide ions investigated. Parallel binding studies were done *in crystallo* on single crystals of the artificial Cu proteins. Spectroscopic changes in solution are consistent with azide binding to the Cu centers. Structural studies corroborate that a Cu–N_3 unit is present in each Sav subunit and reveal the composition of hydrogen bonding (H-bonding) networks that include the coordinated azido ligand. The networks involve amino acid residues and water molecules within the secondary coordination sphere. Mutation of these residues to ones that cannot form H-bonds caused a measurble change in the equilibrium binding constants that were measured in solution. These findings further demonstrate the utility of biotin–Sav technology to prepare water-stable inorganic complexes whose structures can be controlled within both primary and secondary coordination spheres.

The development of functional inorganic complexes has often relied on the regulation of the primary coordination sphere, in which control of key properties such as Lewis acidity and electronic structure can be achieved through variations in the ligands that are covalently coordinated to the metal center(s). It is now recognized that the local environment, the volume of space immediately surrounding metal complexes that comprises the secondary coordination sphere, also affects the function of metal complexes.[1–4] The effects of the secondary coordination sphere are best observed from structure–function studies on the active sites of metalloproteins, in which the modulation of physical properties range from redox potentials and pK_a values, to regulation of structural properties such as the availability of open binding sites.[5] Control within the secondary coordination sphere is often achieved through non-covalent interactions, especially H-bonds. These findings have sparked examination of the structural features necessary to control the secondary coordination sphere

[†]Electronic supplementary information (ESI) available: Experimental details, Fig. S1–S13, and Tables S1–S5. See DOI: 10.1039/c8cc01931b

Correspondence to: A. S. Borovik.

Conflicts of interest
Authors declare no competing financial interest.

Author Manuscript Author Manuscript Author Manuscript Author Manuscript

within molecular species. Our group and others have developed synthetic systems in which the structure of the ligands enforces formation of intramolecular H-bonds.[6–13] For instance, we have established design concepts for ligands that install H-bond donors and acceptors proximal to a metal center to synthesize complexes with terminal hydroxido and oxido ligands.[3,4]

Artificial metalloproteins (ArMs) provide another approach that can be used to probe the effects of local environments surrounding metal ions and there are now numerous methods to prepare ArMs.[14–19] Biotin–streptavidin (biotin–Sav) technology has been found to be an effective method for producing ArMs and there are important examples in which incorporation of biotinylated organometallic complexes within Sav have produced artificial metalloenzymes that are highly selective.[20] Most systems have focused on catalytic function and thus the role of secondary coordination sphere is often inferred from reactivity and selectivity studies. Moreover, the binding of external ligands or substrates is rarely directly observed, especially from X-ray diffraction (XRD) methods.

Recently, we demonstrated that biotin–Sav technology can be used to design active sites that mimic many of the physical properties found for Type I Cu sites in cupredoxins, which are proteins that have a central role in biological electron transfer.[21] This work established design principles to produce active sites that contain metal complexes with unusual primary coordination spheres. We have also established that Sav can be used to stabilize reactive Cu^{II}–OOH species through H-bonds within the local environment provided by Sav WT.[22] In the work described in this report, we further explore the utility of H-bonding network in ArMs to regulate the binding of an external azido ligand through control of the secondary coordination sphere. Investigations done in solution and *in crystallo* provide evidence that modulation of the secondary coordination sphere is achieved through two synergistic effects: (1) the surrounding amino acid residues from the protein host and (2) the length of the linker in the biotinylated metal complex that places the Cu center in specific locations within Sav.

The starting point for our study was the $[Cu^{II}(\text{biot-et-dpea})(H_2O)_2]^{2+}\subset$Sav WT (**1**, dpea, di[2-(2-pyridyl)ethyl]amine, Fig. 1) ArM that we previously showed contains mononuclear Cu(II) complexes within each subunit of Sav.[21] The molecular structure of **1** (PDB 5WBC) shows the Cu(II) center with nearly trigonal bipyramidal coordination geometry (Fig. S1 and Table S1, ESI†) with three N-atom donors from the dpea ligand. The remaining two sites contain two O-atom donors from coordinated water molecules, in which the ligand containing O3 is also H-bonded to O1, a structural water molecule that is present in all our Sav WT structures (Fig. S1, ESI†).[21,22] We have also prepared $[Cu^{II}(\text{biot-pr-dpea})(H_2O)_2]^{2+}\subset$Sav WT (**2**) that contains a similar immobilized Cu(II) complex but has a propyl group between biotin and the dpea moiety, rather than an ethyl group as used in **1** (Fig. 2A, Fig. S2, and Table S1, ESI†). The change in spacer group places the Cu(II) complex farther from the biotin binding site toward the subunit interface. This change in positioning produced a substantial structural change in the secondary coordination sphere with O1 no longer directly interacting with the aqua ligand of the complex. A new H-bonding network is

†Electronic supplementary information (ESI) available: Experimental details, Fig. S1–S13, and Tables S1–S5. See DOI: 10.1039/c8cc01931b

Author Manuscript Author Manuscript Author Manuscript Author Manuscript

observed in **2** that is more extensive than in **1**. The ligand containing O2 forms a H-bond with water molecule (O4) which further interacts with other water molecules within the active site (including O1). Only weak density was observed for a second aqua ligand in the trigonal plane and therefore was not modelled.‡ These structural results supports the premise that the position of the metal complexes within Sav can be regulated using different linker groups which also affects the complex's secondary coordination sphere.[21]

ArMs **1** and **2** provided the opportunity to examine the effects of binding external ligands to the immobilized Cu complexes. We chose to study the binding of azide ions to **1** and **2** to examine changes in both the primary and secondary coordination spheres of Cu centers. Cu(II)–N_3 complexes are known to exhibit a strong azido-to-Cu(II) charge transfer (LMCT) band that can be used to follow ligand binding in solution.[12,23–27] Azide ions bind to the immobilized Cu(II) centers *via* treating **1** and **2** with up to a 40-fold excess of NaN_3 at pH = 6 to produce **1**-N_3 and **2**-N_3 (Fig. 2B and Fig. S3, Table S2, ESI†). The optical spectra for **1**-N_3 (Fig. 2B) and **2**-N_3 (Fig. S3, ESI†) contained a new peak at λ_{max} = 390 nm that is assigned to the LMCT transition. Commensurate changes in the dd bands were observed that are similar to those reported for related Cu–N_3 complexes.[12,27] In addition, the circular dichroism (CD) spectra for **1**-N_3 and **2**-N_3 showed strong bands associated with the LMCT transitions that support that the optical transitions arise from species in a chiral environment enforced by the protein host (Fig. S4, ESI†). As expected, no CD signals were observed for free Cu(II)–N_3 complexes in solution without Sav. The optical properties and EPR parameters of **1**-N_3 and **2**-N_3 are thus consistent with the formation of monomeric Cu(II)–N_3 centers within Sav WT in solution (Fig. S5, S6 and Tables S2, S3, ESI†).

The molecular structures of the Cu complexes in **1**-N_3 and **2**-N_3 were determined using XRD methods. *In crystallo* preparations of **1**-N_3 and **2**-N_3 involved incubating single crystals of **1** and **2** with a 1.0 mM solution of NaN_3 at pH = 6 that resulted in the color of the crystals to change from blue to green (Fig. 3A and B). The molecular structure of **1**-N_3 was solved to 1.37 Å resolution to find a single four-coordinate Cu(II) complex housed within each subunit of Sav (Fig. 3B). The dpea ligand is again bound in a meridional orientation with an average Cu–N_{dpea} bond length of 2.07(3) Å (Table S1, ESI†). Weak electron density (<3σ) was observed in the $F_0 - F_c$ omit map position of the aqua ligand (O2 in **1**, see ESI† and Fig. S1) and was therefore not included in our depiction of **1**-N_3.‡ The electron density of the fourth ligand (Fig. 3D) was accurately modeled as three-atom unit that is assigned to a terminally coordinated azido ligand with a Cu–N4 bond distance of 1.88(3) Å: these metrical parameters are similar to those reported for other Cu(II)–N_3 complexes.[12,27,28]

One of the striking features about the structure of **1**-N_3 is the H-bonding network that surrounds the Cu–N_3 unit. An overlay of **1** and **1**-N_3 (Fig. 3E) shows that the Cu(dpea) fragments in both ArMs are positioned in a similar location within Sav. The structural comparison indicates that binding of the azide ion displaces the aqua ligand (O3) that was present in **1**. This specific coordination site places the ligand inward, toward the biotin binding site and in position to form H-bonds.

‡The aqua ligand is likely displaced due to photoreduction of the sample during data collection. We have shown previously, however, that the photoreduction does not significantly affect the metrical parameters for the remaining ligands (see ESI†).[22]

Author Manuscript Author Manuscript Author Manuscript Author Manuscript

In **1**, an H-bond is formed between the aqua ligand (O3) and the structural water (O1); in **1**-N_3, H-bonds are present between the proximal and second N-atoms of the azido ligand and O1 with N4· · ·O1 and N5· · ·O1 distances of 3.2 and 3.3 Å (Fig. 3C). In addition, a third H-bond is found in **1**-N_3 involving the distal N-atom of the azido ligand and the residue of N49 with an N6· · ·N7 distance of 2.7 Å.

This H-bond network extends beyond the azido–N49 interaction. The carboxylate sidechain of E51 is H-bonded to HN_ε of R84, positioning $H_2N_{\eta 2}$ of R84 to donate an H-bond to the carbonyl of the N49 side chain. This network locks the orientation of N49, suggesting that it donates an H-bond from the HN_δ of the amide group to N6 of the azido ligand (Fig. S7, ESI†). The extended H-bonding network that included N49, R84, and E51 is not limited to **1**-N_3, as it is also found within biotin–Sav WT. Insights into the structural changes that produce this H-bonding network were obtained from comparison of the reported structures of Sav WT and biotin–Sav WT.[29] Residues 45–52 form a flexible loop that sits in an open conformation in apo-Sav but closes upon binding within the biotin binding site (Fig. S8, ESI†). Upon biotin binding, residue N49 moves ~10 Å and its amide backbone, along with the S45 sidechain, H-bond to biotin. This movement causes the loop to close over biotin and thus orienting residues N49 and E51 on either side of R84, fixing the position of all three residues.[29]

The molecular structure of **2**-N_3 was solved to 1.45 Å and showed also a monomeric Cu complex within each subunit that has a geometry between trigonal bipyramidal and square pyramidal (τ_5 = 0.52, Fig. 4 and Table S1, ESI†).[§]30 The distorted square plane is composed of the two N-atom donors from the pyridyl groups of dpea, an O-atom donor from an aqua ligand (O2), and an N-atom donor from the terminal azido ligand.[¶] The primary coordination sphere is completed by the amine N-atom of dpea that occupies the axial position. The metrical parameters (Table S1, ESI†) are consistent with this assignment in which the O2–Cu–N4 bond angle is 147(4)° and Cu–N4 and Cu–O2 bond lengths are 1.87(3) and 2.29(3) Å. Compared to **1**-N_3, the Cu center in **2**-N_3 is located approximately 2 Å further from the biotin binding site toward the adjacent subunit. This change in location is attributed to the lengthening of the linker group to a propyl unit as discussed for **2** (see above). The Cu complex in **2**-N_3 is far enough from N49 and O1 that the azido ligand can no longer H-bond with them. Instead, the azido ligand occupies a coordination site on the Cu center (relative to **2**, see Fig. 2A) that allows it to form a single H-bond with residue K121′ with an N6· · ·N7 distance of 2.7 Å. Note that the lysine residue involved in this H-bond is from the adjacent subunit (K121′, Fig. 4). The aqua ligand is also a part of an extended H-bonding network that includes several water molecules but not N49 (Fig. 4).

Equilibrium binding constants (*K*) were determined to further investigate the effects of the H-bonding networks on the confinement of the Cu(II)–N_3 complexes (Table S2, ESI†). In addition to measuring the equilibrium constants for **1**-N_3 and **2**-N_3, we studied azide ion binding to three other variants: $[Cu^{II}(\text{biot-et-dpea})(H_2O)_2]^{2+}\subset$Sav N_{49}A (**1a**), $[Cu^{II}(\text{biot-et-dpea})\text{-}(H_2O)_2]^{2+}\subset$Sav S_{112}A (**1b**), and $[Cu^{II}(\text{biot-pr-dpea})(H_2O)_2]^{2+}\subset$Sav K_{121}A (**2a**). We

[§]For an ideal trigonal bipyramid coordination geometry τ_5 = 1 and for an ideal square pyramidal coordination geometry τ_5 = 0.
[¶]The azido ligand in **2**-N_3 was refined with 50% occupancy.

Author Manuscript Author Manuscript Author Manuscript Author Manuscript

reasoned that these changes would alter the H-bonds to the azido ligand which could affect its binding. Equilibrium studies were done spectrophotometrically (Fig. S9–S11, ESI†) by monitoring the changes in the LMCT band of the Cu(II)–N_3 complexes (see ESI†).[26] These studies also produced Hill coefficients (Fig. S10 and S11, ESI†) that indicated a 1 : 1 binding of azide ion to each Cu(II) complex, results that are consistent with non-cooperative, terminal ligand coordination (Table S2, ESI†). An $K = 23 \pm 4\ M^{-1}$ was measured for the formation of **1**-N_3 that decreased to an $K = 6 \pm 2\ M^{-1}$ for **1a**-N_3 and an $K = 12 \pm 2\ M^{-1}$ for **1b**-N_3. A smaller, but statistically significant, trend was found for the variants with $[Cu^{II}(biot\text{-}pr\text{-}dpea)]^{2+}$: an $K = 68 \pm 5\ M^{-1}$ was obtained for **2**-N_3 that decreased to $K = 56 \pm 3\ M^{-1}$ in **2a**-N_3.

The trend in equilibrium constants within each variant support the premise that H-bonds within the secondary coordination spheres influence azide ion binding. For the variants with $[Cu^{II}(biot\text{-}et\text{-}dpea)]^{2+}$, the equilibrium constant was reduced by nearly a factor of 4 when the H-bonding network was changed *via* the mutation of N_{49}A. This difference corresponds to a change in free energy of approximately 0.8 kcal mol^{-1} which is attributed to the loss of the asparagine residue that donates a H-bond to the distal N-atom of the azido ligand in **1**-N_3. Mutation of S_{112} to alanine in **1b** decreases the occupancy of the structural water molecule,[22,31] O1, which eliminates the bifurcated H-bond to the proximal and second N-atoms in the azido ligand. The disruption of this H-bond causes a 2-fold decrease in equilibrium constant, corresponding to a ~0.4 kcal mol^{-1} change in free energy. The binding constants for the ArMs are comparable to those reported for synthetic Cu(II) complexes in water that range from 10–289 M^{-1};[26] however, the structures of these synthetic complexes were not obtained. Additionally, larger values are found for variants with **2** than **1** (Table S2, ESI†) which we suggest is caused by the Cu center being anchored further from the biotin binding site and thus more accessible to exogenous ligands.

The monitoring of azide binding to the Cu complexes within **1** and **2** provide insights into the design of protein active sites. Our work showed that H-bonding networks can be utilized to regulate the secondary coordination spheres around confined metal complexes using biotin–Sav technology. Using an approach that combined ligand binding in solution and *in crystallo* structural investigations allowed us to correlate changes in molecular structure with equilibrium binding constants. We discovered that the residue N_{49} and a structural water molecule provide a natural local environment to form H-bonds to external species such as azido or peroxido[22] ligands on $[Cu^{II}(biot\text{-}et\text{-}dpea)]^{2+}$. This H-bonding network was made possible in part because the Cu(II) complexes were positioned relatively near the biotin-binding site through the use of an ethylene spacer. When a longer spacer group was utilized in **2**-N_3, the Cu(II) complex was positioned farther from the biotin-binding site that resulted in a different H-bonding network around the azido ligand along with a change in coordination geometry of the Cu. This change in geometry is a result of microenvironment provided by the protein host. These findings further demonstrate the important consequences of positioning metal complexes at different locations within the Sav host. Additional structural tuning was accomplished through mutagenesis of Sav to modulate the secondary coordination sphere. Single mutations to the amino acids involved in H-bond formation in both **1** and **2** produced smaller azide binding constants in solution, highlighting the effects of

Author Manuscript Author Manuscript Author Manuscript Author Manuscript

the H-bonds in regulating the properties in ArMs. Our findings further establish the design principles needed to control the secondary coordination spheres around metal ions using biotin–Sav technology.

Supplementary Material

Refer to Web version on PubMed Central for supplementary material.

Acknowledgments

Acknowledgement is made to the NIH (GM120349 to ASB and GM50781-21S1 to ASB and TRW) for financial support and the UCI Laser Spectroscopy Facility.

References

1. Shook RL, Borovik AS. Inorg Chem. 2010; 49:3646–3660. [PubMed: 20380466]
2. Shook RL, Borovik AS. Chem Commun. 2008:6095.
3. Cook SA, Borovik AS. Acc Chem Res. 2015; 48:2407–2414. [PubMed: 26181849]
4. Cook SA, Hill EA, Borovik AS. Biochemistry. 2015; 54:4167–4180. [PubMed: 26079379]
5. Lu Y, Valentine JS. Curr Opin Struct Biol. 1997; 7:495–500. [PubMed: 9266170]
6. Momenteau M, Reed CA. Chem Rev. 1994; 94:659–698.
7. Ogo S, Wada S, Watanabe Y, Iwase M, Wada A, Harata M, Jitsukawa K, Masuda H, Einaga H. Angew Chem, Int Ed. 1998; 37:2102–2104.
8. Garner DK, Allred RA, Tubbs KJ, Arif Atta M, Berreau LM. Inorg Chem. 2002; 41:3533–3541. [PubMed: 12079475]
9. Garner DK, Fitch SB, McAlexander LH, Bezold LM, Arif Atta M, Berreau LM. J Am Chem Soc. 2002; 124:9970–9971. [PubMed: 12188644]
10. Natale D, Mareque-Rivas JC. Chem Commun. 2008:25–437.
11. MAreque-Rivas JC. Curr Org Chem. 2007; 11:1434–1449.
12. Wada A, Honda Y, Yamaguchi S, Nagatomo S, Kitagawa T, Jitsukawa K, Masuda H. Inorg Chem. 2004; 43:5725–5735. [PubMed: 15332825]
13. Jitsukawa K, Oka Y, Yamaguchi S, Masuda H. Inorg Chem. 2004; 43:8119–8129. [PubMed: 15578852]
14. Dürrenberger M, Ward TR. Curr Opin Chem Biol. 2014; 19:99–106. [PubMed: 24608081]
15. Petrik ID, Liu J, Lu Y. Curr Opin Chem Biol. 2014; 19:67–75. [PubMed: 24513641]
16. Lewis JC. Curr Opin Chem Biol. 2015; 25:27–35. [PubMed: 25545848]
17. Yu F, Cangelosi VM, Zastrow ML, Tegoni M, Plegaria JS, Tebo AG, Mocny CS, Ruckthong L, Qayyum H, Pecoraro VL. Chem Rev. 2014; 114:3495–3578. [PubMed: 24661096]
18. Cavazza C, Bochot C, Rousselot-Pailley P, Carpentier P, Cherrier MV, Martin L, Marchi-Delapierre C, Fontecilla-Camps JC, Ménage S. Nat Chem. 2010; 2:1069–1076. [PubMed: 21107372]
19. Berggren G, Adamska A, Lambertz C, Simmons TR, Esselborn J, Atta M, Gambarelli S, Mouesca JM, Reijerse E, Lubitz W, Happe T, Artero V, Fontecave M. Nature. 2013; 498:66–69.
20. Heinisch T, Ward TR. Acc Chem Res. 2016; 49:1711–1721. [PubMed: 27529561]
21. Mann SI, Heinisch T, Weitz AC, Hendrich MP, Ward TR, Borovik AS. J Am Chem Soc. 2016; 138:9073–9076. [PubMed: 27385206]
22. Mann SI, Heinisch T, Ward TR, Borovik AS. J Am Chem Soc. 2017; 139:17289–17292. [PubMed: 29117678]
23. Pate JE, Ross PK, Thamann TJ, Reed CA, Karlin KD, Sorrell TN, Solomon EI. J Am Chem Soc. 1989; 111:5198–5209.
24. Karlin KD, Cohen BI, Hayes JC, Farooq A, Zubieta J. Inorg Chem. 1987; 26:147–153.
25. Casella L, Gullotti M, Pallanza G, Buga M. Biol Met. 1990; 3:137–140.

Author Manuscript Author Manuscript Author Manuscript Author Manuscript

26. Casella L, Gullotti M, Pallanza G, Buga M. Inorg Chem. 1991; 30:221–227.
27. Lee DH, Murthy NN, Karlin KD. Inorg Chem. 1997; 36:5785–5792. [PubMed: 11670200]
28. Rahaman SH, Ghosh R, Lu TH, Ghosh BK. Polyhedron. 2005; 24:1525–1532.
29. Freitag S, Le Trong I, Klumb L, Stayton PS, Stenkamp RE. Protein Sci. 1997; 6:1157–1166. [PubMed: 9194176]
30. Addison AW, Rao TN, Reedijk J, van Rijn J, Verschoor GC. J Chem Soc, Dalton Trans. 1984:1349–1356.
31. Dürrenberger M, Heinisch T, Wilson YM, Rossel T, Nogueira E, Knörr L, Mutschler A, Kersten K, Zimbron MJ, Pierron J, Schirmer T, Ward TR. Angew Chem, Int Ed. 2011; 50:3026–3029.

Author Manuscript Author Manuscript Author Manuscript Author Manuscript

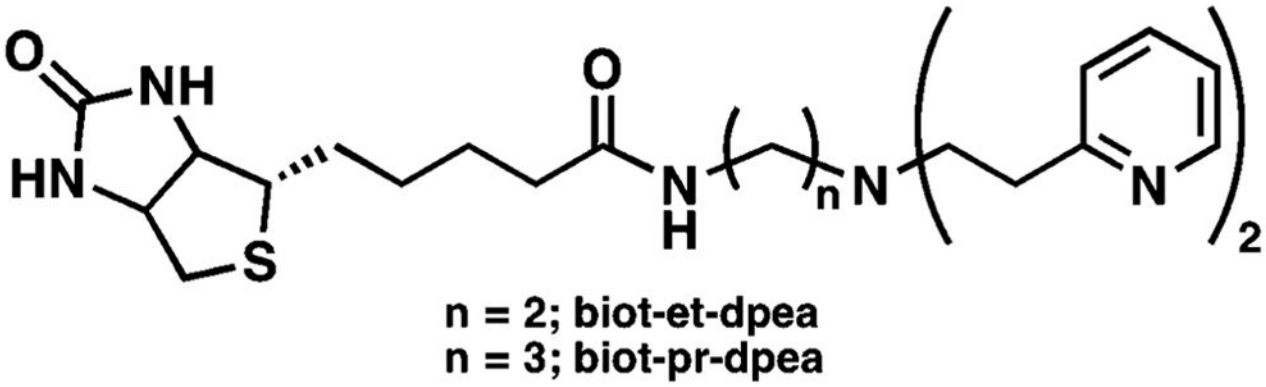

Fig. 1.
Biotinylated ligands used in this study.

Author Manuscript Author Manuscript Author Manuscript Author Manuscript

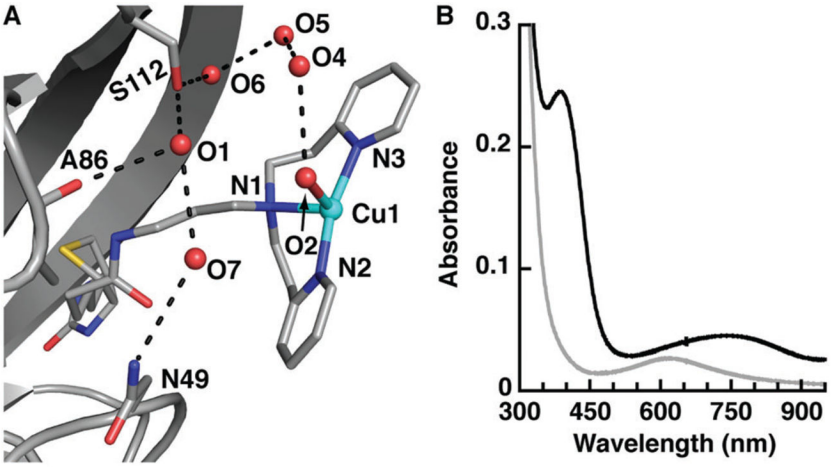

Fig. 2.

The molecular structure of **2** (A) and the absorbance spectra for **1** (grey) and **1**-N_3 (black) (B). Dashed lines indicate H-bonds. O2· · ·O4, 3.14(2) Å; O4· · ·O5, 2.60(2) Å; O5· · ·O6, 3.07(2) Å; O1· · ·O7, 3.20(2) Å.

Author Manuscript Author Manuscript Author Manuscript Author Manuscript

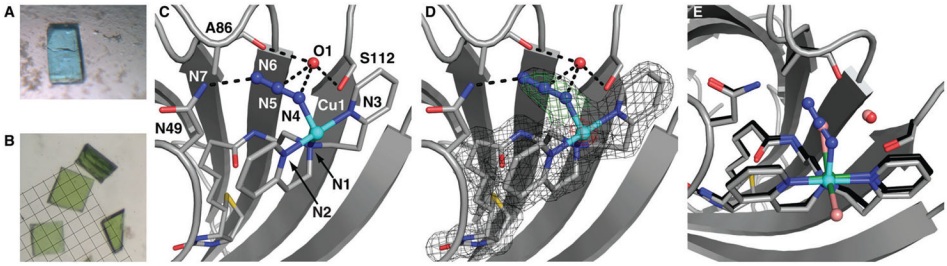

Fig. 3.

Photographs comparing crystals of **1** (A) and **1**-N_3 (B), the molecular structure of **1**-N_3 (C & D), and structural overlay of **1** and **1**-N_3 (E). For the structure in D the position of the complex is indicated by the $2F_0 - F_c$ electron density (grey, contoured at 1σ), anomalous difference density (red, contoured at 15σ) and the azido ligand position is indicated with $F_0 - F_c$ omit map (green, contoured at 3σ). Cu-ions are colored in cyan, N-atoms are colored in blue, and O-atoms/water molecules are colored in red. H-Bonds are displayed as dashed black lines. In (E), **1** is shown with C-atoms in black, N-atoms in blue, O-atoms/water molecules in salmon, and Cu-ions in green.

Author Manuscript Author Manuscript Author Manuscript Author Manuscript

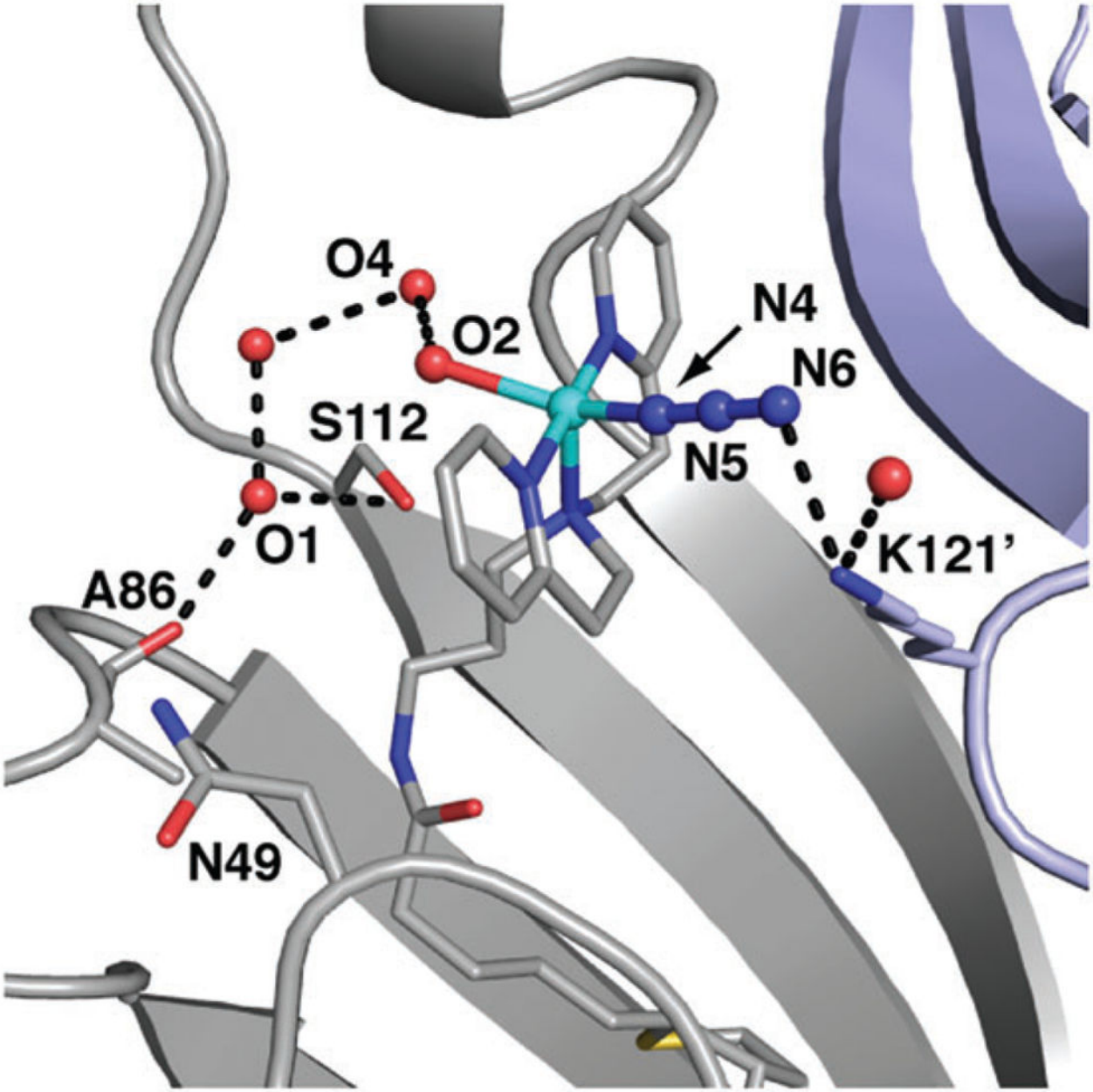

Fig. 4.

Molecular structure of **2**-N_3 showing the primary coordination sphere and including the extended H-bonding network. Dashed lines indicate H-bonds. K121′ is from the adjacent subunit (shown in light blue). Cu-Ions are in cyan, N-atoms are in blue, and O-atoms/water molecules are in red.